Journal of Organometallic Chemistry 897 (2019) 70–79

Contents lists available at ScienceDirect

Journal of Organometallic Chemistry

journal homepage: www.elsevier.com/locate/jorganchem

Gold(I)-catalyzed [4 + 1]/[4 + 3] annulations of diazo esters with hexahydro-1,3,5-triazines: Theoretical study of mechanism and regioselectivity

Luo-yi Zhou, Xian-ming Guo, Zhong-chao Zhang, Juan Li*

Department of Chemistry, Jinan University, Huangpu Road West 601, Guangzhou, Guangdong, 510632, PR China

ARTICLE INFO

Article history:
Received 5 May 2019
Received in revised form
19 June 2019
Accepted 24 June 2019
Available online 25 June 2019

Keywords:
Transition metal
Density functional theory
[4 + 1]/[4 + 3] cycloaddition
C–H activation
Regioselectivity
Mechanism

ABSTRACT

Hexahydro-1,3,5-triazines are often used as formaldimine precursors. The recent success of Sun et al. (*Angew. Chem. Int. Ed.*, 2016, **55**, 11867) in achieving gold-catalyzed [4 + 1]/[4 + 3] annulations of hexahydro-1,3,5-triazines with diazo esters, in which the hexahydro-1,3,5-triazine is directly used as the 1,4-dipole in the annulation, represents a breakthrough in mechanistic studies. In the present work, density functional theory (DFT) calculations were used for detailed investigation of possible catalytic mechanisms. The proposed catalytic cycle involves five major stages: dinitrogen elimination to form a gold–carbene intermediate; diazoacetate–hexahydro-1,3,5-triazine C–C coupling to give an ammonium ylide; ring opening of the hexahydro-1,3,5-triazine via C–N single-bond cleavage; a second C–N single-bond cleavage; and C–C-bond-forming reductive elimination. The regioselectivities of the cycloaddition of hexahydro-1,3,5-triazines with enol diazoacetates differ from those of cycloadditions with vinyl diazoacetates. The calculations also clarified the origins of the substrate-controlled regioselectivity.

1. Introduction

Diazo compounds are essential reactants in various organic transformations [1]. In recent years, transition-metal-catalyzed intermolecular reactions of diazo compounds with readily available substrates have provided a powerful strategy for constructing various carbocycles and heterocycles [2]. Diazo compounds can serve as efficient one-to three-carbon synthons, mainly through metallocarbene formation [3]. Metal-mediated carbene transfer reactions from diazo reagents are generally catalyzed by rhodium [4] or copper [5]. However, the use of gold complexes in such reactions has been less well investigated, although the reactivities and selectivities of gold-mediated carbene transfer reactions often differ greatly from those of similar reactions catalyzed by copper, rhodium, and other metals [6].

Hexahydro-1,3,5-triazines have been used as stable precursors of formaldimines in aminomethylation and hydroaminomethylation reactions by incorporating the aminomethyl group into a functionalized molecule [7]. Sun and coworkers have reported a novel gold-catalyzed [4 + 1]/[4 + 3] annulation of hexahydro-1,3,5-triazines with diazo esters in which the hexahydro-1,3,5-triazine is directly used as the 1,4-dipole in the annulation (Scheme 1) [8]. Their work represents a breakthrough in mechanistic investigations. The hexahydro-1,3,5-triazines react directly with gold carbenes rather than as formaldimine precursors. Sun et al. also showed that cycloaddition of hexahydro-1,3,5-triazines with diazo esters proceeds with high regioselectivity, despite the existence of competing carbenic and vinylogous position (Scheme 2).

The theoretical studies of the reaction mechanism of gold(I)-catalyzed carbene transfer from diazo compounds are rare. Recently, a combined theoretical and experimental study on the mechanism of the gold-catalyzed [2 + 2+1] annulation of aryldiazo nitriles and two imines was reported [9]. DFT calculations have been conducted to unravel the mechanisms and chemoselectivities of Au(I)-catalyzed couplings of phenyl diazoacetate with phenyl unsaturated aliphatic alcohols [10]. However, the detailed mechanism of hexahydro-1,3,5-triazine as the 1,4-dipole to couple with diazo compound have not yet been reported. Consequently, we used DFT calculations to clarify the mechanism and the origin of the regioselectivity of gold-catalyzed [4 + 1]/[4 + 3] annulation of hexahydro-1,3,5-triazines with diazo esters.

* Corresponding author.
E-mail address: tchjli@jnu.edu.cn (J. Li).

https://doi.org/10.1016/j.jorganchem.2019.06.032
0022-328X/

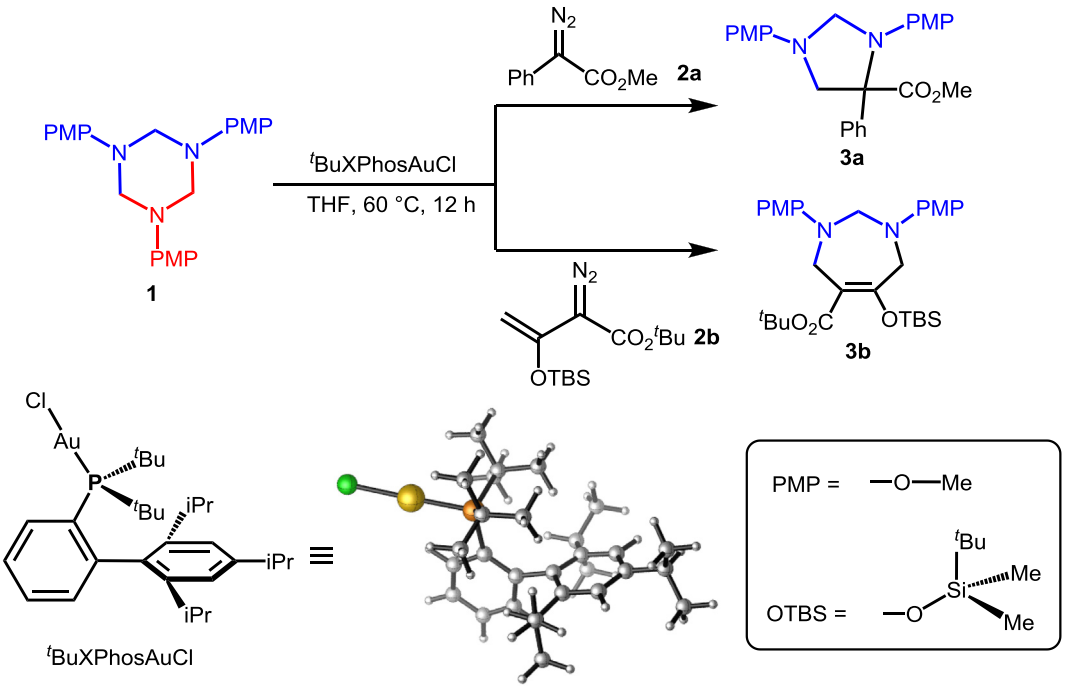

Scheme 1. Gold-catalyzed [4 + 1]/[4 + 3] annulation of hexahydro-1,3,5-triazine with diazo ester.

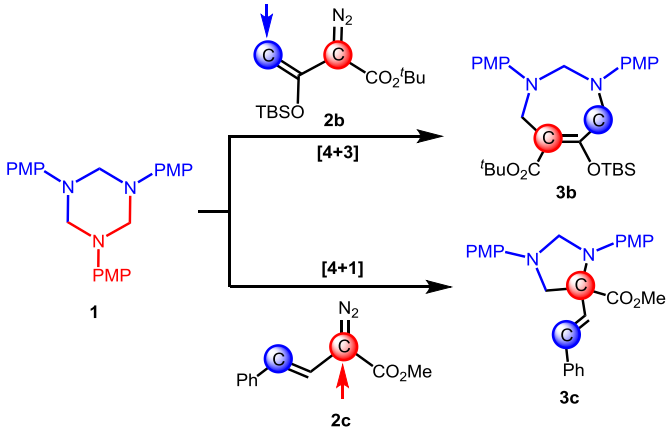

Scheme 2. Regioselectivity of gold-catalyzed [4 + 1]/[4 + 3] annulation.

2. Computational details

All stationary points were optimized without any constraints in the solvent phase at the B3LYP level of theory [11], which has been shown to describe Au-catalyzed organometallic systems reasonably well [10,12]. Solvent effects were treated with the SMD solvation model [13], with tetrahydrofuran as the solvent. All calculations were performed with the Gaussian 09 quantum chemical program [14]. Frequency calculations at the same level of theory were also performed to identify all the stationary points as minima (zero imaginary frequencies) or transition states (one imaginary frequency), and to calculate the free energies at 333.15 K. Intrinsic reaction coordinate calculations were performed to verify the transition-state structures [15]. In this analysis, the Au atom was described by the LANL2DZ basis set, including a double-valence basis set with the Hay and Wadt effective core potential [16]. Polarization functions were added for Au ($\zeta_f = 1.050$) [17]. The 6-31G* [18] basis set was used for other atoms. This basis set combination will be referred to as BS1. To obtain more accurate energy information, all energies were corrected by single-point calculations at the M06 level with a larger basis set (BS2) [19]. Empirical D3 dispersion corrections were included for the M06 functional [20]. BS2 utilizes LANL2TZ(f) [21] for Au and 6−311++G** for other atoms.

To assess how sensitive our results are to the dispersive effects for geometry optimizations, the structures of some key transition states were reoptimized at the B3LYP-D3/BS1 level, and then their relative energies were re-evaluated with single-point calculations using the M06-D3/BS2 level of theory. Using the M06-D3/BS2//B3LYP/BS1 calculations, the relative energies of **TS2B**, **TS3B′**, **TS3C**, and **TS5C′** are −38.0, −35.4, −27.1, and −24.2 kcal/mol, respectively. Using the M06-D3/BS2//B3LYP-D3/BS1 calculations, the relative Gibbs energies are −37.2, −34.6, −26.7, and −23.5 kcal/mol, respectively. Our calculations indicate that M06-D3/BS2//B3LYP/BS1 and M06-D3/BS2//B3LYP-D3/BS1 predicted similar results and led to the same discussion and conclusions.

3. Results and discussion

Widenhoefer and co-workers [22] suggested that only cationic gold intermediates were involved in gold-carbene related transformations by the comprehensive NMR study. Furthermore, DFT calculations [9,10,12,23] offer strong support for gold cation taking part as active catalyst in the gold(I)-catalyzed reactions. Therefore, it should be reasonable for us to consider the $[^t\text{BuXPhosAu}]^+$ as the active species that coordinates to the substrate initiating the reaction. We used hexahydro-1,3,5-triazine **1** with phenyl diazoacetate (**2a**) as a representative system (Scheme 1) for clarifying the novel reaction mechanism (section 3.1). On the basis of the established mechanism, we investigated the regioselectivities for enol and vinyl diazoacetates (sections 3.2 and 3.3). For each transition state and intermediate, we searched all possible conformers by adjusting the flexible rotating bonds and minimizing them to the lowest conformers, while fixing the rigid backbone of the molecule.

3.1. Mechanism of direct reaction of hexahydro-1,3,5-triazine with metal carbene

As shown in Scheme 3, phenyl diazoacetate (**2a**) initially coordinates to the gold center of the active catalyst, i.e., [^{t}BuXPhosAu]$^+$, via carbon to form intermediate **1A**, which is exergonic by 5.2 kcal/mol. The **1A** C1–N bond is longer than that in the isolated diazo compound **1** (i.e., 1.317 Å for **1** versus 1.388 Å for **1A**; atom numbering is shown in the schemes and figs.). This indicates that the diazo compound is weakly coordinated to the Au center in **1A**. The following step is formation of the gold–carbene **2A** via dinitrogen elimination. The free energy of the denitrogenation transition state **TS1A** was determined to be 1.4 kcal/mol (Scheme 3). Formation of Au–carbene **2A** increases the exergonicity to 27.4 kcal/mol, which indicates that the dinitrogen elimination steps are highly energetically favorable. The geometries show that the Au–C1 distance in **TS1A** is only slightly shorter, by 0.116 Å, than that in **1A**, and is further shortened to 2.033 Å in **2A**.

Fig. 1 shows the pathways starting from **2A**, together with the energetic results. Fig. 2 shows the optimized structures of the key stationary points labeled in Fig. 1. As shown by the red line in Fig. 1, hexahydro-1,3,5-triazine **1** first approaches **2A** to give **3A′**. Diazoacetate–hexahydro-1,3,5-triazine C–C coupling then takes place via **TS2A′** and leads to **4A′**. The calculated free energy of transition state **TS2A′** is −31.5 kcal/mol. We then performed calculations for C–N bond formation with the assistance of a second gold atom (black line in Fig. 1). Hexahydro-1,3,5-triazine **1**, which is coordinated to a second Au, becomes involved, to afford intermediate **3A**. Then **3A** completes the C–N bond via transition state **TS2A**, with a small energy barrier of −0.7 kcal/mol (Fig. 1). The free energy of **TS2A**, which is formed with the assistance of a second gold, is 1.3 kcal/mol lower than that of **TS2A′**, which is formed via a mono-gold pathway. This shows the importance of the second gold in facilitating the reaction. In **4A**, the C1–N1 distance of 1.658 Å indicates C1–N1 bond formation. The C2–N1 and C4–N1 bonds in **4A** are longer than those in hexahydro-1,3,5-triazine **1** (i.e., 1.462 and 1.468 Å for **1** versus 1.549 and 1.535 Å for **4A**). This confirms that **4A** has ammonium ylide characteristics. This is further supported by natural bond orbital (NBO) charge analysis. The calculated atomic charge on the N1 atom in **4A** (−0.317) is more positive than that on N1 in **1** (−0.510).

The gold atom then undergoes ligand exchange to give **5A**. In **5A**, the C1–N1, C1–C5, and C5–O1 distances are 1.594, 1.492, and 1.251 Å, respectively; compared to those in **4A**, the C5–O1 distance is longer, and the C1–N1 and C1–C5 distances are shorter. These distance changes indicate that isomerization of **4A**–**5A** facilitates the next step, i.e., C–N single-bond cleavage. The next step is ring opening of the hexahydro-1,3,5-triazine via C–N single-bond cleavage to give **6A**, which has an energy barrier of 6.2 kcal/mol (**TS3A**) relative to **4A**. In **TS3A**, the C2–N2 and C1–N1 distances are changed to 1.335 and 1.534 Å, respectively, and that of the breaking C2–N1 bond is 2.079 Å. We also performed calculations for ring opening of the hexahydro-1,3,5-triazine with a mono-gold catalyst. The DFT calculations show that the mono-gold pathway has an energy barrier of 8.4 kcal/mol (**TS3A′**), which is 2.2 kcal/mol higher than that for the di-gold pathway. This suggests that ring opening of the hexahydro-1,3,5-triazine with a mono-gold catalyst is still unfavorable.

The iminium ylide **6A** is more stable than the ammonium ylide **5A** by 11.1 kcal/mol. In **6A**, the C2–N2 and C3–N2 distances are 1.280 and 1.581 Å; this provides direct evidence of an iminium ylide. The isomerization of iminium ylide **6A** to **6A-iso** by coordination of the C2 atom to one gold center is impossible because **6A** is 22.8 kcal/mol more stable than **6A-iso**. This implies that the presence of the ylide intermediate in the reaction pathway is essential. The iminium ylide **6A** is then converted to the ylide intermediate **7A** via a second C–N single-bond cleavage, with dissociation of formaldimine **4**. The process **6A** → **7A** is facile and has an energy barrier of 9.8 kcal/mol (**TS4A**). The geometric structure of the **TS4A** transition state indicates C3–N2 single-bond cleavage, with a calculated C3···N2 distance of 2.128 Å. The di-gold and mono-gold mechanisms were compared to assess the favorability of the di-gold mechanism for the second C–N single-bond cleavage. The results show that the energy of **TS4A′** is higher than that of **TS4A**, by about 1.6 kcal/mol, therefore in the preferred reaction the second C–N single-bond cleavage involves the di-gold catalyst rather than the mono-gold catalyst.

The second Au catalyst then dissociates to afford **8A**. The C1–C5 distance decreases from 1.488 to 1.383 Å and the C5–O1 distance increases from 1.254 to 1.294 Å from **7A** to **8A**; this suggests that the binding of gold with the O1 atom switches from the η [2] to the η [1] mode. The shortening of the distance between the C1 atom and C5 atom from **7A** to **8A** promotes subsequent formation of the C1–C3 bond. Then C–C-bond-forming reductive elimination takes place, leading to intermediate **9A**. The located transition state (**TS5A**) shows that the C1···C3 distance is 2.417 Å. The predicted energy barrier for this step is 23.4 kcal/mol relative to **7A**. Finally, the catalyst is regenerated with concomitant release of the desired product **3a**. From point of view based on an energetic span model [24], **6A** is the TOF-determining intermediate (TDI) and **TS5A** is the TOF-determining transition state (TDTS), which results in an energetic span of 27.8 kcal/mol.

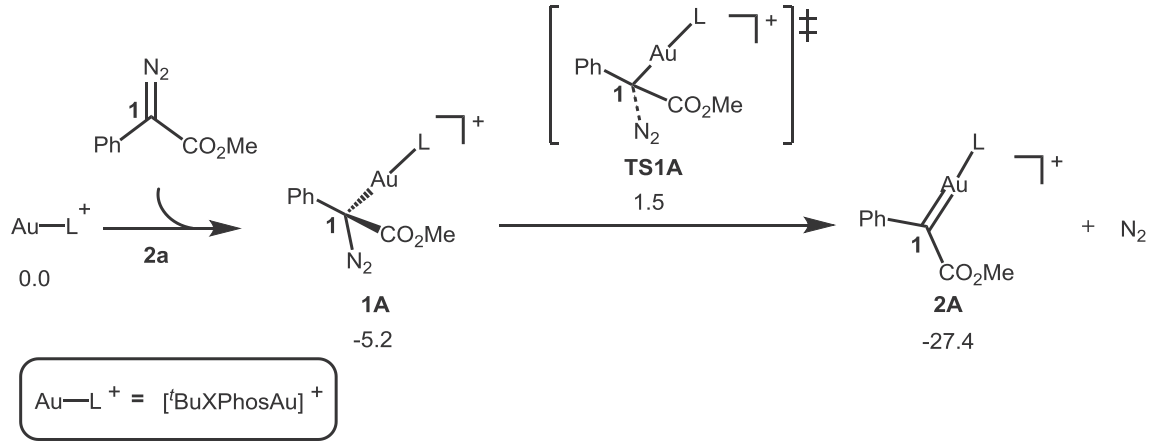

Scheme 3. Mechanism for formation of 2A (free energies are given in kcal/mol).

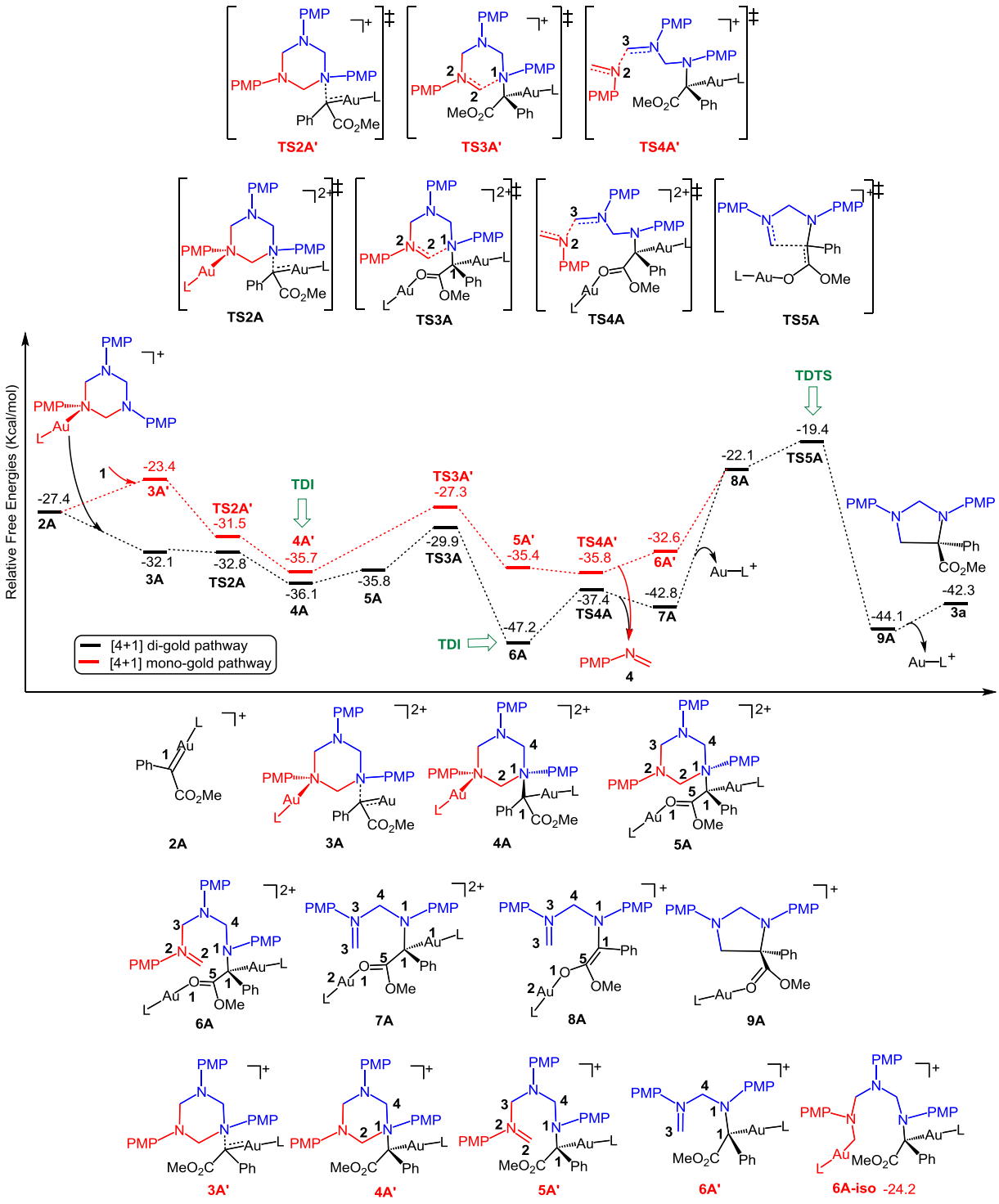

Fig. 1. Calculated free-energy profiles for steps starting from 2A for substrate 2a. Values shown are relative free energies in kcal/mol. Favored pathway is shown in black; other, less favorable, pathway is shown in red. TDI and TDTS are also shown. (For interpretation of the references to colour in this figure legend, the reader is referred to the Web version of this article.)

For the two C–N bond cleavage steps (**4A** → **7A**), a concerted process is also possible, in which both steps occur simultaneously (Scheme 4). However, the free energy of the concerted transition state **TS6A** is much less favorable, by 35.0 kcal/mol, than that of **TS3A**, which is the highest energy point along the two-step successive process. A concerted process (**4A** → **9A**) is also possible in which two C–N bond cleavage steps and C–C bond formation occur simultaneously (Scheme 4). However, the energy barrier (83.9 kcal/mol) for the concerted process via **TS7A** is too high to be accessible.

3.2. Computational investigation of regioselectivity

The starting point for the various mechanistic options that give products **3b** or **3b′** is the gold–enolcarbene intermediate **2B**. The

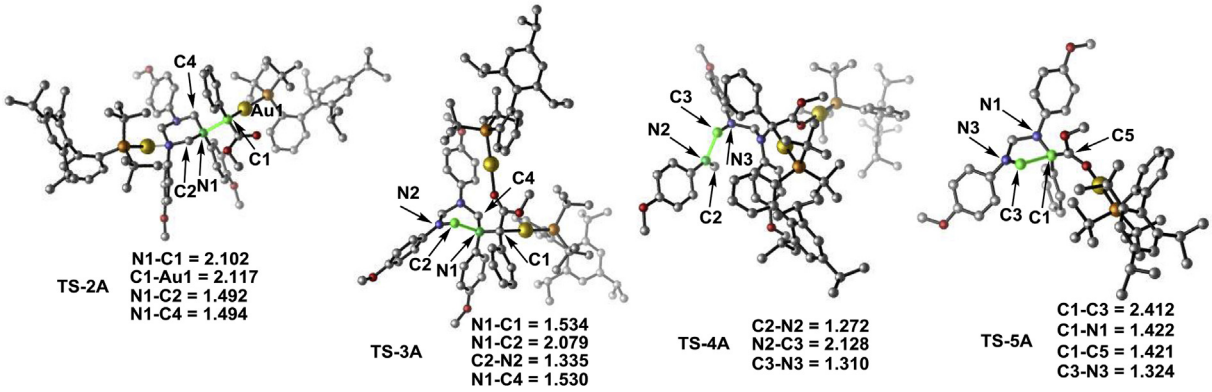

Fig. 2. Optimized structures of key transition states labeled in Fig. 1. Key bond lengths are given in Å; trivial H atoms are omitted for clarity.

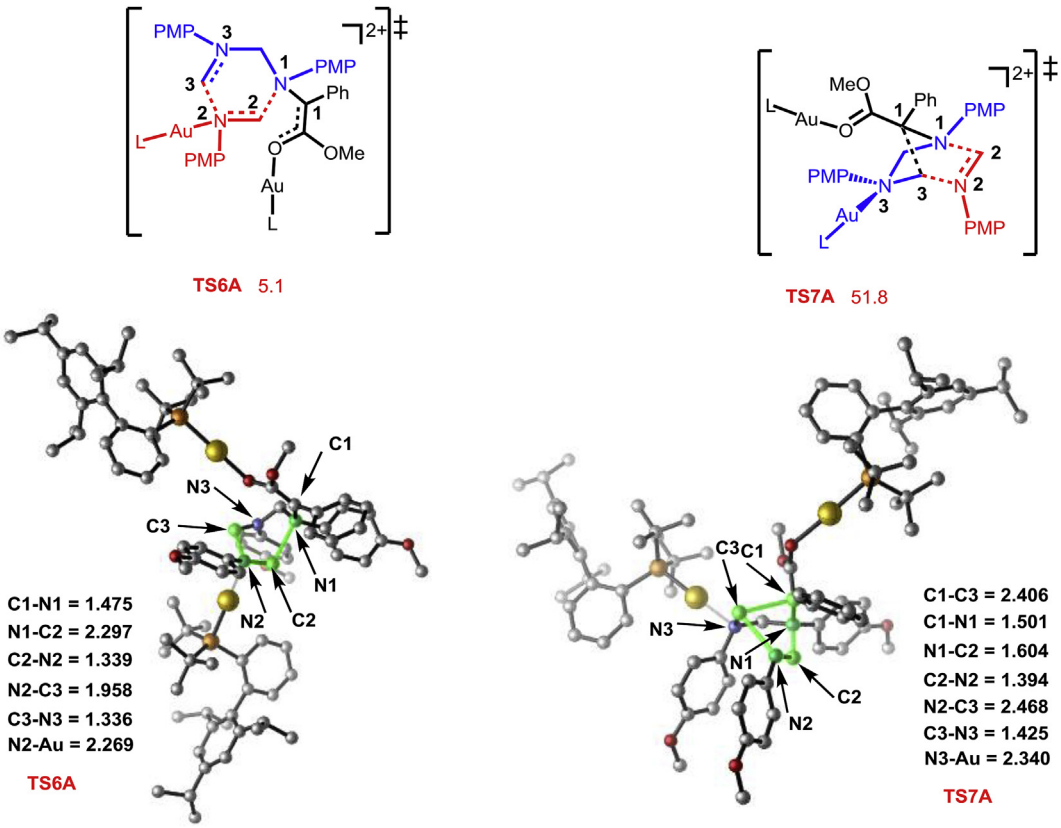

Scheme 4. Structures of concerted transition states TS6A and TS7A with free energies in kcal/mol.

addition of hexahydro-1,3,5-triazine **1**–**2B** can take place on either the carbenic ([4 + 1] annulation) or vinylogous ([4 + 3] annulation) position. The NBO charges on the carbenic C1 and vinylogous C3 in **2B** are −0.141 and −0.242, respectively. It can be concluded that C1 is more electrophilic than C3 in **2B**, therefore the difference between the charge distributions does not control the regioselectivity. We therefore decided to explore the factors that control the regioselectivity. Fig. 3 compares the structural evolutions along the two potential regiodivergent pathways. The black line leads to [4 + 3] annulation via attack at the vinylogous position, and the red line generates a [4 + 1] annulation product via attack at the carbenic position. The calculated energy profiles along other possible pathways are given in Fig. S1 in the electronic supplementary information.

Along the black line, the first step is an intermolecular nucleophilic process, in which the nitrogen atom in the hexahydro-1,3,5-triazine nucleophilically attacks the C3 atom in **2B**. The process via **TS2B** is facile with a free-energy barrier of 0.8 kcal/mol; it provides the stable ammonium ylide **4B**, in which the positive charge on the gold is transferred to the hexahydro-1,3,5-triazine nitrogen atom. This is supported by the NBO charge on the N1 atom, which increases to −0.315 in **4B** from −0.461 in **3B**. Step **4B** → **5B** involves a simple conformational change from η [2]-N2 coordination with Au(I) (the Au–N2 bond length is 2.296 Å) to η [2]-O1 coordination (the Au–O1 bond length is 2.189 Å). This step is necessary for subsequent ring opening of the hexahydro-1,3,5-triazine. The transition state for breakage of the C–N bond is **TS3B**, in which the N1···C4 distance increases to 2.301 Å. The calculated free-energy

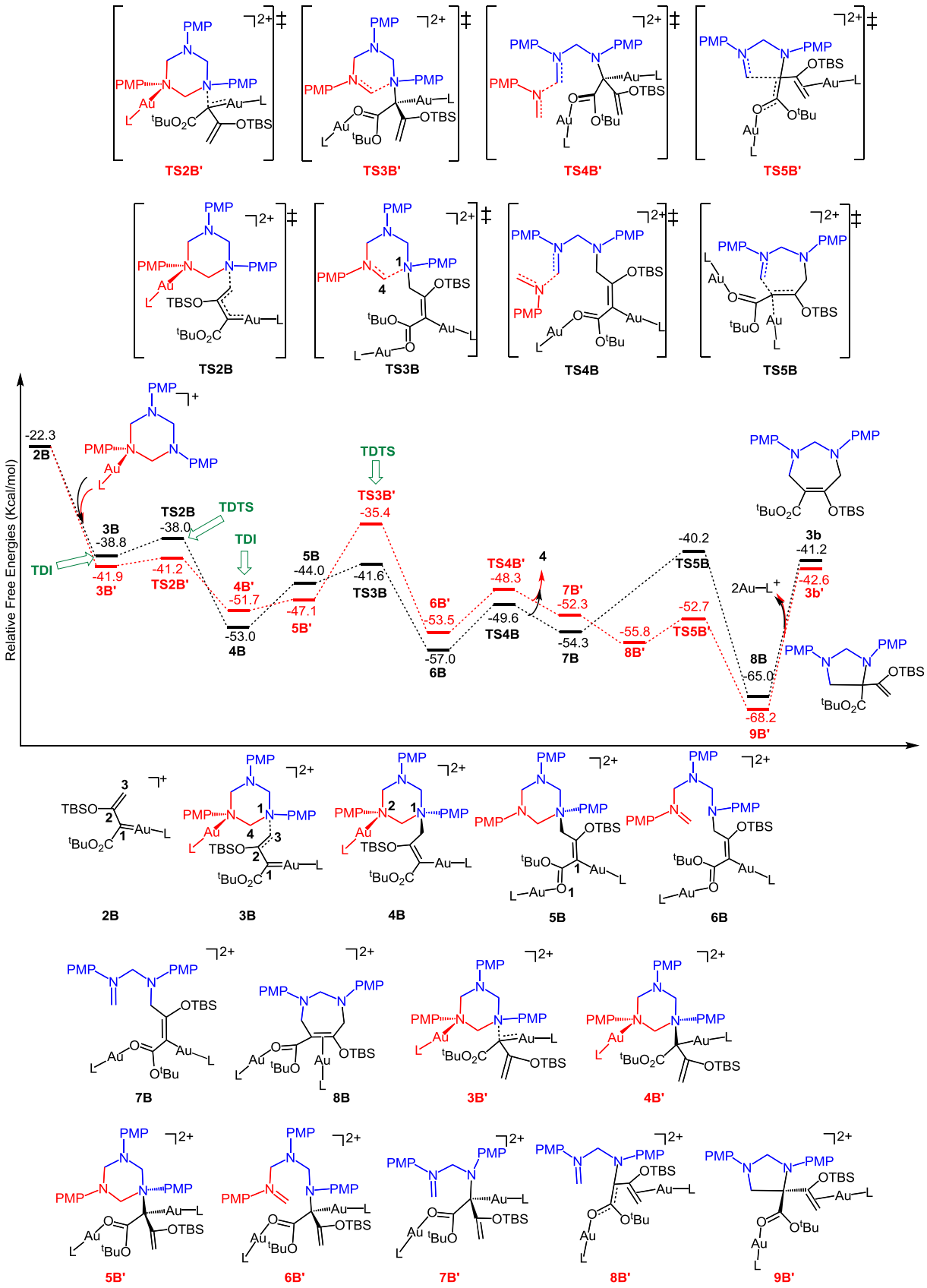

Fig. 3. Calculated free-energy profiles for steps starting from 2B for substrate 2b. Values shown are relative free energies in kcal/mol. Major [4 + 3] annulation pathway is shown in black; regioisomeric [4 + 1] annulation pathway is shown in red. TDI and TDTS are also shown. (For interpretation of the references to colour in this figure legend, the reader is referred to the Web version of this article.)

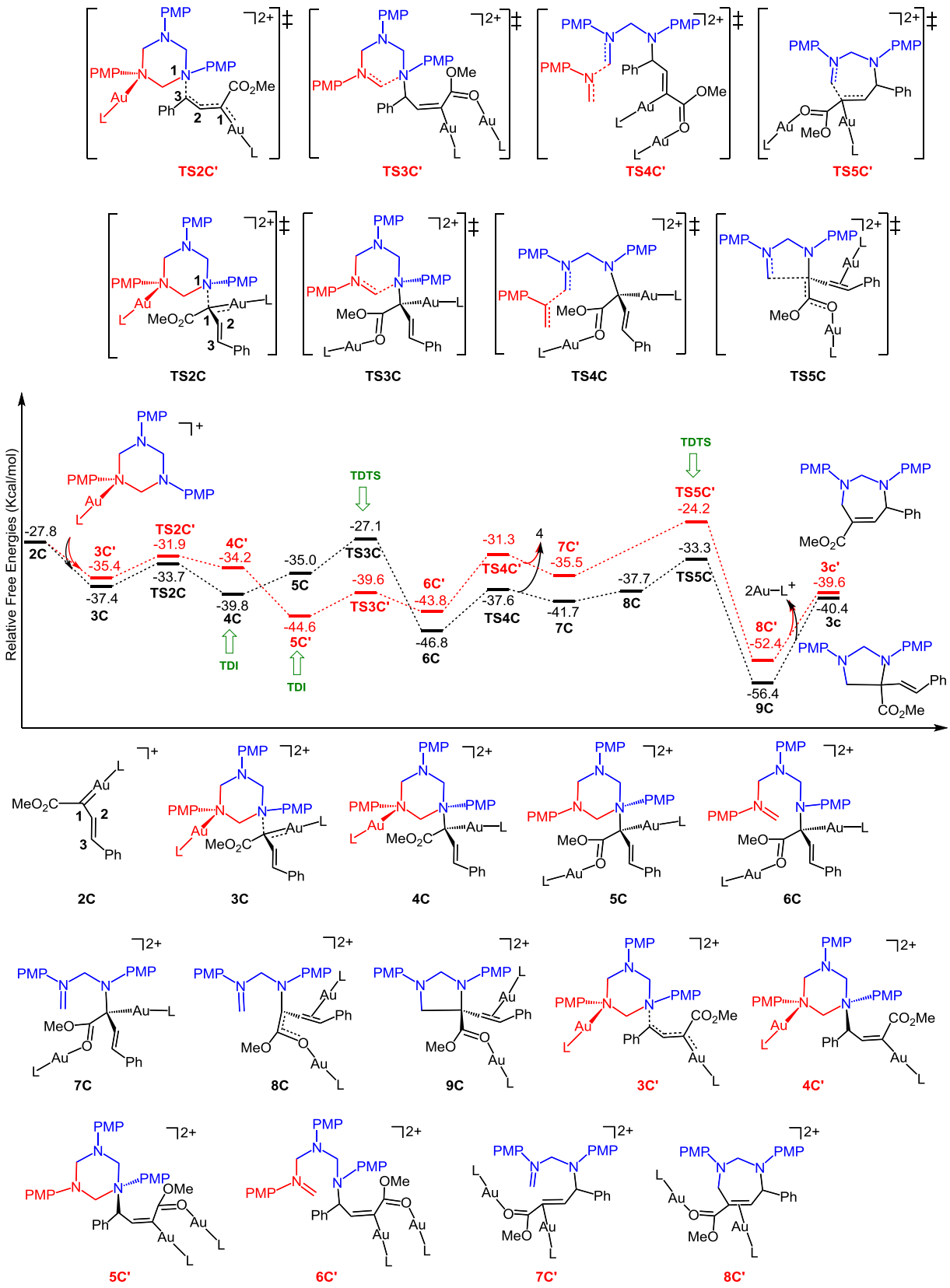

Fig. 4. Calculated free-energy profiles for steps starting from 2C for substrate 2c. Values shown are relative free energies in kcal/mol. Major [4 + 1] annulation pathway is shown in black; regioisomeric [4 + 3] annulation pathway is shown in red. TDI and TDTS are also shown. (For interpretation of the references to colour in this figure legend, the reader is referred to the Web version of this article.)

barrier for the ring-opening reaction is 11.4 kcal/mol. After formation of **6B**, a second C–N bond breakage occurs via transition state **TS4B**, with a free-energy barrier of 7.4 kcal/mol. This leads to the ylide intermediate **7B**, which is unstable (−54.3 kcal/mol) relative to **6B**. This iminium ylide can evolve into the stable seven-membered heterocyclic intermediate **8B** via **TS5B**, with an activation-energy barrier of 14.1 kcal/mol with respect to **7B**.

Along the red line, the [4 + 1] annulation reaction for **2b** follows similar mechanisms to those for **2a**, which were discussed in section 3.1. The relevant mechanistic details are therefore not discussed again, for simplicity. The reaction involves four elementary steps: diazoacetate–hexahydro-1,3,5-triazine C–C coupling (**3B′** → **4B′**) via transition state **TS2B′**; ring opening of the hexahydro-1,3,5-triazine through C–N single-bond cleavage (**4B′** → **6B′**) via **TS3B′**; a second C–N single-bond cleavage (**6B′** → **8B′**) via **TS4B′**; and C–C-bond-forming reductive elimination (**8B′** → **9B′**) via **TS5B′**. The **TS2B** and **TS3B′** transition states correspond to the highest energy points along the [4 + 3] and [4 + 1] annulation reactions, respectively. **TS3B′** is energetically less favorable, by 2.5 kcal/mol, than **TS2B**. In kinetic terms, it is therefore understandable that no [4 + 1] annulation was observed for enol diazoacetates by Sun and coworkers [8]. Although nucleophilic attack of the carbenic C1 (**TS2B′**) is favored over attack of the vinylogous C3 (**TS2B**), which is supported by the NBO charge analysis, the following ring-opening transition state **TS3B** is more favorable than **TS3B′**. This can be explained by the presence of an important conjugation effect in **TS3B**, which is absent in **TS3B′**.

Next, we performed calculations on the regioselectivity of the vinyl diazoacetate substrate. The potential energy profiles for forming the [4 + 1] annulation product **3c** and [4 + 3] annulation product **3c′** are shown in Fig. 4; these are all based on the optimal reaction pathway. The calculated energy profiles along other possible pathways are given in Fig. S2 in the electronic supplementary information. Fig. 4 shows that once the gold–carbene species **2C** is obtained, the 1,2,3-triazole attacks the carbenic center of **2C** or the vinylogous C3, via **TS2C** or **TS2C′**, to form a C1–N1 or C3–N1 covalent bond, respectively. The diazoacetate-hexahydro-1,3,5-triazine C–C coupling spans an energy barrier of 3.7 or 3.5 kcal/mol and gives nitrogen ylide **4C** or **4C′**, respectively. Ring opening of the 1,2,3-triazole occurs by spanning a low barrier, i.e., 7.9 or 5.0 kcal/mol (**TS3C** or **TS3C′**), leading to **6C** or **6C′**, respectively. A second C–N breakage through **TS4C** or **TS4C′** results in formation of ylide species **7C** or **7C′** and release of formaldimine **4**. The steps following formation of intermediate **7C** or **7C′** are associated with generation of a five-membered or seven-membered heterocycle. The transformation from **7C** to **8C** involves ligand exchange from η [1]-C1 coordination with Au(I) to η [2]-C2=C3 coordination with Au(I); this favors subsequent C1–C4 bond formation. Finally, reductive elimination gives the five-membered or seven-membered heterocycle **3c** or **3c′** via transition state **TS5C** or **TS5C′**, respectively. The overall reaction free-energy profile indicates that **TS3C** and **TS5C′** are the regiodivergence-determining transition states, and their calculated relative energies are −27.1 and −24.3 kcal/mol, respectively. The energy of **TS5C′** is higher than that of **TS5C** for the C–C-bond-forming step. This can be attributed to η [2]-C2=C3 coordination with Au(I) in **TS5C**, which is absent in **TS5C′**.

On the basis of the energy profiles shown in Fig. 3, we can conclude that the [4 + 3] annulation pathway for enol diazoacetate is kinetically favored over the [4 + 1] annulation pathway. For the vinyl diazoacetate, as shown in Fig. 4, the [4 + 1] annulation pathway is kinetically favored over the [4 + 3] annulation pathway. These results are consistent with experimental observations [8], which showed that the enol diazoacetate gave mainly the [4 + 3] annulation product, whereas the vinyl diazoacetate gave mainly the [4 + 1] annulation product. The difference between the enol diazoacetate and vinyl diazoacetate systems can be attributed to the significant differences between the C–C-bond-forming reductive elimination steps. The energy barrier in the reductive-elimination step for the vinyl diazoacetate is much higher than that for the enol diacetate; this ultimately makes [4 + 3] annulation unfavorable. The electron-donating –OTBS substituent on the enol diazoacetate lowers the reductive-elimination barrier and makes [4 + 3] annulation favorable. The presence of the –OTBS substituent on the enol diazoacetate is therefore crucial to the feasibility of the [4 + 3] annulation.

4. Conclusions

The gold-catalyzed [4 + 1]/[4 + 3] annulation of hexahydro-1,3,5-triazines with diazo esters, which was reported by Sun and coworkers, represents a breakthrough in mechanistic investigations. In their reaction, the hexahydro-1,3,5-triazine is directly used as a 1,4-dipole for the annulation rather than as a formaldimine precursor. We performed a DFT study to determine the novel reaction mechanism. Our results show, for the first time, that the annulation of hexahydro-1,3,5-triazines with diazo esters involves five steps: (a) dinitrogen elimination to form a gold–carbene intermediate; (b) diazoacetate–hexahydro-1,3,5-triazine C–C coupling to give an ammonium ylide; (c) ring opening of the hexahydro-1,3,5-triazine via C–N single-bond cleavage; (d) a second C–N single-bond cleavage; and (e) C–C-bond-forming reductive elimination.

The other significant insight provided by the result so of this work is the origin of the regioselectivities for enol diazoacetates and vinyl diazoacetates. The experimental results, which show that regiodivergent annulation can give two different products with highly selectivity, were reasonably reproduced by the DFT calculations. The regioselectivity for [4 + 3] annulation of the enol diazoacetate is controlled by the conjugation effects in the ring opening of the hexahydro-1,3,5-triazine. The coordination of a double bond to gold in the reductive elimination step plays an important role in the regioselectivity for the [4 + 1] annulation of vinyl diazoacetate.

Conflicts of interest

There are no conflicts to declare.

Acknowledgements

This work was supported by the National Natural Science Foundation of China (Grant No. 21573095), the Science and Technology Program of Guangzhou (Grant No. 201707010269), and the high-performance computing platform at Jinan University.

Appendix A. Supplementary data

Supplementary data to this article can be found online at https://doi.org/10.1016/j.jorganchem.2019.06.032.

References

[1] For selected books and reviews, see (a) M.P. Doyle, M.A. McKervey, T. Ye, Modern Catalytic Methods for Organic Synthesis with Diazo Compounds, vol. 2, Wiley, New York, 1998, pp. 393–399;
(b) A. Padwa, M.D. Weingarten, Cascade processes of metallo carbenoids, Chem. Rev. 96 (1996) 223–270;
(c) D.M. Hodgson, A.H. Labande, S. Muthusamy, Cycloadditions of carbonyl ylides derived from diazocarbonyl compounds, Org. React. 80 (2013) 133–496;
(d) M. Marinozzi, F. Pertusati, M. Serpi, λ^5-Phosphorus-containing α-diazo

compounds: a valuable tool for accessing phosphorus-functionalized molecules, Chem. Rev. 116 (2016) 13991–14055;
(e) N.R. Candeias, R. Paterna, P.M.P. Gois, Homologation reaction of ketones with diazo compounds, Chem. Rev. 116 (2016) 2937–2981;
(f) L. Liu, J. Zhang, Gold-catalyzed transformations of α-diazocarbonyl compounds: selectivity and diversity, Chem. Soc. Rev. 45 (2016) 506–516.

[2] For reviews, see (a) M.P. Doyle, R. Duffy, M. Ratnikov, L. Zhou, Catalytic carbene insertion into C–H bonds, Chem. Rev. 110 (2010) 704–724;
(b) Y. Xia, Y. Zhang, J. Wang, Catalytic cascade reactions involving metal carbene migratory insertion, ACS Catal. 3 (2013) 2586–2598;
(c) A. Ford, H. Miel, A. Ring, C.N. Slattery, A.R. Maguire, M.A. McKervey, Modern organic synthesis with α-diazocarbonyl compounds, Chem. Rev. 115 (2015) 9981–10080;
(d) J. Barluenga, C. Valds, Tosylhydrazones: new uses for classic reagents in Palladium-catalyzed cross-coupling and metal-free reactions, Angew. Chem. Int. Ed. 50 (2011) 7486–7500;
(e) Z. Shao, H. Zhang, N-tosylhydrazones: versatile reagents for metal-catalyzed and metal-free cross-coupling reactions, Chem. Soc. Rev. 41 (2012) 560–572;
(f) Q. Xiao, Y. Zhang, J. Wang, Diazo compounds and N-tosylhydrazones: novel cross-coupling partners in transition-metal-catalyzed reactions, Acc. Chem. Res. 46 (2013) 236–247;
(g) G. Qin, L. Li, J. Li, H. Huang, Palladium-catalyzed formal insertion of carbenoids into aminals via C–N bond activation, J. Am. Chem. Soc. 137 (2015) 12490–12493.

[3] For reviews, see (a) H.M.L. Davies, J.R. Denton, Application of donor/acceptor-carbenoids to the synthesis of natural products, Chem. Soc. Rev. 38 (2009) 3061–3071;
(b) H.M.L. Davies, D. Morton, Guiding principles for site selective and stereoselective intermolecular C–H functionalization by donor/acceptor Rhodium carbenes, Chem. Soc. Rev. 40 (2011) 1857–1869;
(c) X. Zhao, Y. Zhang, J. Wang, Recent developments in Copper-catalyzed reactions of diazo compounds, Chem. Commun. 48 (2012) 10162–10173;
(d) X. Xu, M.P. Doyle, The [3 + 3]-cycloaddition alternative for heterocycle syntheses: catalytically generated metalloenolcarbenes as dipolar adducts, Acc. Chem. Res. 47 (2014) 1396–1405;
(e) S. Zhu, Q. Zhou, Transition-metal-catalyzed enantioselective heteroatomhydrogen bond insertion reactions, Acc. Chem. Res. 45 (2012) 1365–1377;
(f) Z. Zhang, J. Wang, Recent studies on the reactions of α-diazocarbonyl compounds, Tetrahedron 64 (2008) 6577–6605;
(g) H. Lebel, J.F. Marcoux, C. Molinaro, A.B. Charette, Stereoselective cyclopropanation reactions, Chem. Rev. 103 (2003) 977–1050;
(h) Q. Cheng, M.P. Doyle, Chapter one-The selection of catalysts for metal carbene transformations, Adv. Organomet. Chem. 66 (2016) 1–31;
(i) N.J. Thumar, Q. Wei, W. Hu, Chapter two-Recent advances in asymmetric metal-catalyzed carbene transfer from diazo compounds toward molecular complexity, Adv. Organomet. Chem. 66 (2016) 33–91.

[4] For selected examples, see (a) A.G. Smith, H.M. Davies, Rhodium-catalyzed enantioselective vinylogous addition of enol ethers to vinyldiazoacetates, J. Am. Chem. Soc. 134 (2012) 18241–18244;
(b) J.E. Spangler, H.M.L. Davies, Catalytic asymmetric synthesis of pyrroloindolines via a Rhodium(II)-catalyzed annulation of indoles, J. Am. Chem. Soc. 135 (2013) 6802–6805;
(c) P.E. Guzmán, Y. Lian, H.M.L. Davies, Reversal of the regiochemistry in the Rhodium-catalyzed [4+3] cycloaddition between vinyldiazoacetates and dienes, Angew. Chem. Int. Ed. 53 (2014) 13083–13087;
(d) P.Q. Le, J.A. May, Hydrazone-initiated carbene/alkyne cascades to form polycyclic products: ring-fused cyclopropenes as mechanistic intermediates, J. Am. Chem. Soc. 137 (2015) 12219–12222;
(e) S.K. Alamsetti, M. Spanka, C. Schneider, Synergistic Rhodium/phosphoric acid catalysis for the enantioselective addition of oxonium ylides to ortho-quinone methides, Angew. Chem. Int. Ed. 55 (2016) 2392–2396;
(f) R.A. Panish, S.R. Chintala, J.M. Fox, A mixed-ligand chiral Rhodium(II) catalyst enables the enantioselective total synthesis of piperarborenine B, Angew. Chem. Int. Ed. 55 (2016) 4983–4987;
(g) J. Kalepu, S. Katukojvala, Dienamine activation of diazoenals: application to the direct synthesis of functionalized 1,4-oxazines, Angew. Chem. Int. Ed. 55 (2016) 7831–7835;
(h) Q. Cheng, J. Yedoyan, H. Arman, M.P. Doyle, Dirhodium(II)-catalyzed annulation of enoldiazoacetamides with α-diazoketones: an efficient and highly selective approach to fused and bridged ring systems, Angew. Chem. Int. Ed. 55 (2016) 5573–5576;
(i) X. Wang, X. Xu, P.Y. Zavalij, M.P. Doyle, Asymmeric formal [3 + 3]-cycloaddition reactions of nitrones with electrophilic vinylcarbene intermediates, J. Am. Chem. Soc. 133 (2011) 16402–16405;
(j) X. Xu, Y. Qian, P.Y. Zavalij, M.P. Doyle, Highly selective catalyst-dependent competitive 1,2-C→C, -O→C, and -N→C migrations from β-Methylene-β-silyloxy-β-amido-α-diazoacetates, J. Am. Chem. Soc. 135 (2013) 1244–1247;
(k) X. Xu, P.Y. Zavalij, M.P. Doyle, Highly enantioselective dearomatizing formal [3+3] cycloaddition reactions of N-acyliminopyridinium ylides with electrophilic enol carbene intermediates, Angew. Chem. Int. Ed. 52 (2013) 12664–12668.

[5] For selected examples, see (a) Q. Cheng, J. Yedoyan, H. Arman, M.P. Doyle, Copper-catalyzed divergent addition reactions of enoldiazoacetamides with nitrones, J. Am. Chem. Soc. 138 (2016) 44–47;
(b) S.M. Nicolle, W. Lewis, C.J. Hayes, C.J. Moody, Stereoselective synthesis of highly substituted tetrahydrofurans through diverted carbene O–H insertion reaction, Angew. Chem. Int. Ed. 54 (2015) 8485–8489;
(c) S.M. Nicolle, W. Lewis, C.J. Hayes, C.J. Moody, Stereoselective synthesis of functionalized pyrrolidines by the diverted N–H insertion reaction of metallocarbenes with β-aminoketone derivatives, Angew. Chem. Int. Ed. 55 (2016) 3749–3753;
(d) K. Liu, C. Zhu, J. Min, S. Peng, G. Xu, J. Sun, Stereodivergent synthesis of N-heterocycles by catalyst-controlled, activity-directed tandem annulation of diazo compounds with amino alkynes, Angew. Chem. Int. Ed. 54 (2015) 12962–12967.

[6] (a) V.V. Pagar, R. Liu, Gold-catalyzed cycloaddition reactions of ethyl diazoacetate, nitrosoarenes, and vinyldiazo carbonyl compounds: synthesis of isoxazolidine and benzo[*b*]azepine derivatives, Angew. Chem. Int. Ed. 54 (2015) 4923–4926;
(b) J.F. Briones, H.M.L. Davies, Gold(I)-catalyzed asymmetric cyclopropenation of internal alkynes, J. Am. Chem. Soc. 134 (2012) 11916–11919;
(c) J. Barluenga, G. Lonzi, M. Tomás, L.A. López, Reactivity of stabilized vinyl diazo derivatives toward unsaturated hydrocarbons: regioselective Gold-catalyzed carbon-carbon bond formation, Chem. Eur J. 19 (2013) 1573–1576;
(d) Z. Yu, B. Ma, M. Chen, H. Wu, L. Liu, J. Zhang, Highly site-selective direct C–H bond functionalization of phenols with α-aryl-α-diazoacetates and diazooxindoles via gold catalysis, J. Am. Chem. Soc. 136 (2014) 6904–6907;
(e) Y. Xi, Y. Su, Z. Yu, B. Dong, E.J. McClain, Y. Lan, X. Shi, Chemoselective carbophilic addition of α-diazoesters through ligand-controlled gold catalysis, Angew. Chem. Int. Ed. 53 (2014) 9817–9821;
(f) J. Wang, X. Yao, T. Wang, J. Han, J. Zhang, X. Zhang, P. Wang, Z. Zhang, Synthesis of 2,5-dihydrofurans via a Gold(I)-catalyzed formal [4 + 1] cycloaddition of α-diazoesters and propargyl alcohols, Org. Lett. 17 (2015) 5124–5127;
(g) Z. Yu, H. Qiu, L. Liu, J. Zhang, Gold-catalyzed construction of two adjacent quaternary stereocenters via sequential C–H functionalization and aldol annulation, Chem. Commun. 52 (2016) 2257–2260;
(h) D. Zhang, G. Xu, D. Ding, C. Zhu, J. Li, J. Sun, Gold(I)-catalyzed diazo coupling: strategy towards alkene formation and tandem benzannulation, Angew. Chem. Int. Ed. 53 (2014) 11070–11074;
(i) Y. Liu, Z. Yu, J. Zhang, L. Liu, F. Xia, J. Zhang, Origins of unique Gold-catalysed chemo- and site-selective C–H functionalization of phenols with diazo compounds, Chem. Sci. 7 (2016) 1988–1995;
(j) K. Liu, G. Xu, J. Sun, Gold-catalyzed stereoselective dearomatization/metal-free aerobic oxidation: access to 3-substituted indolines/oxindoles, Chem. Sci. 9 (2018) 634–639.

[7] (a) S. Oda, B. Sam, M.J. Krische, Hydroaminomethylation beyond carbonylation: allene-imine reductive coupling by Ruthenium-catalyzed transfer hydrogenation, Angew. Chem. Int. Ed. 54 (2015) 8525–8528;
(b) S. Oda, J. Franke, M.J. Krische, Diene hydroaminomethylation via Ruthenium-catalyzed C–C bond forming transfer hydrogenation: beyond carbonylation, Chem. Sci. 7 (2016) 136–141;
(c) X. Lian, L. Lin, K. Fu, B. Ma, X. Liu, X. Feng, A new approach to the asymmetric mannich reaction catalyzed by chiral N,N′-dioxide-metal complexes, Chem. Sci. 8 (2017) 1238–1242;
(d) J. Hu, Y. Xie, H. Huang, Palladium-catalyzed insertion of an allene into an aminal: aminomethylamination of allenes by C–N bond activation, Angew. Chem. Int. Ed. 53 (2014) 7272–7276;
(e) S. Liu, P. Yang, S. Peng, C. Zhu, S. Cao, J. Li, J. Sun, Gold-catalyzed sequential annulations towards 3,4-fused bi/tri-cyclic furans involving a [3+2+2]-cycloaddition, Chem. Commun. 53 (2017) 1152–1155;
(f) S. Peng, S. Cao, J. Sun, Gold-catalyzed regiodivergent [2 + 2 + 2]-cycloadditions of allenes with triazines, Org. Lett. 19 (2017) 524–527;
(g) Y. Zheng, Y. Chi, M. Bao, L. Qiu, X. Xu, Gold-catalyzed tandem dual heterocyclization of enynones with 1,3,5-triazines: bicyclic furan synthesis and mechanistic insights, Org. Chem. 82 (2017) 2129–2135;
(h) Z. Zeng, H. Jin, X. Song, Q. Wang, M. Rudolph, F. Rominger, A.S.K. Hashmi, Gold-catalyzed intermolecular cyclocarboamination of ynamides with 1,3,5-triazinanes: en route to tetrahydropyrimidines, Chem. Commun. 53 (2017) 4304–4307;
(k) L.K.B. Garve, P.G. Jones, D.B. Werz, Ring-opening 1-amino-3-aminomethylation of donor-acceptor cyclopropanes via 1,3-diazepanes, Angew. Chem. Int. Ed. 56 (2017) 9226–9230;
(l) D. Ji, C. Wang, J. Sun, Asymmetric [4 + 2]-cycloaddition of Copper-allenylidenes with hexahydro-1,3,5-triazines: access to chiral tetrahydroquinazolines, Org. Lett. 20 (2018) 3710–3713.

[8] C. Zhu, G. Xu, J. Sun, Gold-catalyzed formal [4+1]/[4+3] cycloadditions of diazo esters with triazines, Angew. Chem. Int. Ed. 55 (2016) 11867–11871.

[9] S.K. Pawar, M. Yang, M. Su, R. Liu, Gold-catalyzed oxidative [2+2+1] annulations of aryldiazo nitriles with imines to yield polyarylated imidazolium salts, Angew. Chem. Int. Ed. 56 (2017) 5035–5039.

[10] G. Pei, Y. Liu, G. Chen, X. Yuan, Y. Jiang, S. Bi, Unveiling the mechanisms and secrets of chemoselectivities in Au(I)-catalyzed diazo-based couplings with aryl unsaturated aliphatic alcohols, Catal. Sci. Technol. 8 (2018) 4450–4462.

[11] (a) A.D. Becke, Density-functional thermochemistry. III. The role of exact exchange, J. Chem. Phys. 98 (1993) 5648–5653;
(b) C. Lee, W. Yang, R.G. Parr, Development of the colic-salvetti correlation-energy formula into a functional of the electron density, Phys. Rev. B 37

(1988) 785–789;
(c) P.J. Stephens, F.J. Devlin, C.F. Chabalowski, M.J. Frisch, Ab initio calculation of vibrational absorption and circular dichroism spectra using density functional force fields, J. Phys. Chem. 98 (1994) 11623–11627.

[12] (a) Y. Liu, D. Zhang, S. Bi, C. Liu, Theoretical investigation on Pt(II)- and Au(I)-mediated cycloisomerizations of propargylic 3-indoleacetate: [3 + 2]- versus [2 + 2]-cycloaddition products, Org. Biomol. Chem. 11 (2013) 336–343;
(b) Y. Liu, X. Yang, L. Liu, H. Wang, S. Bi, Mechanistic insight into water-modulated cycloisomerization of enynyl esters using an Au(I) catalyst, Dalton Trans. 44 (2015) 5354–5363;
(c) E. Lopez, J. Gonzalez, L.A. Lopez, Unusual regioselectivity in the Gold(I)-catalyzed [3+2] carbocycloaddition reaction of vinyldiazo compounds and N-allenamides, Adv. Synth. Catal. 358 (2016) 1428–1432;
(d) C. Wang, X. Ren, C. Qi, H. Yu, Mechanistic study on Gold-catalyzed highly selective hydroamination of alkylidenecyclopropanes, J. Org. Chem. 81 (2016) 7326–7335;
(e) F. Shi, X. Li, Y. Xia, L. Zhang, Z. Yu, DFT study of the mechanisms of in water Au(I)-catalyzed tandem [3,3]-rearrangement/nazarov reaction/[1,2]-hydrogen shift of enynyl acetates: a proton-transport catalysis strategy in the water-catalyzed [1,2]-hydrogen shift, J. Am. Chem. Soc. 129 (2007) 15503–15512;
(f) L. Yang, R. Fang, Mechanism of Gold(I)-catalyzed double migration-benzannulation cascade toward naphthalenes: deprotonation/protonation mediated by water, J. Mol. Catal. A Chem. 379 (2013) 197–206;
(g) P. Mauleón, J.L. Krinsky, F.D. Toste, Mechanistic studies on Au(I)-catalyzed [3,3]-sigmatropic rearrangements using cyclopropane probes, J. Am. Chem. Soc. 131 (2009) 4513–4520;
(h) Y. Liu, D. Zhang, S. Bi, Theoretical investigation on the isomerization reaction of 4-phenyl-hexa-1,5-enyne catalyzed by homogeneous Au catalysts, J. Phys. Chem. A 114 (2010) 12893–12899.

[13] A.V. Marenich, C.J. Cramer, D.G. Truhlar, Performance of SM6, SM8, and SMD on the SAMPL1 test set for the prediction of small-molecule solvation free energies, J. Phys. Chem. B 113 (2009) 4538–4543.

[14] M.J. Frisch, G.W. Trucks, H.B. Schlegel, G.E. Scuseria, M.A. Robb, J.R. Cheeseman, G. Scalmani, V. Barone, B. Mennucci, G.A. Petersson, H. Nakatsuji, M. Caricato, X. Li, H.P. Hratchian, A.F. Izmaylov, J. Bloino, G. Zheng, J.L. Sonnenberg, M. Hada, M. Ehara, K. Toyota, R. Fukuda, J. Hasegawa, M. Ishida, T. Nakajima, Y. Honda, O. Kitao, H. Nakai, T. Vreven, J.A. Montgomery Jr., J.E. Peralta, F. Ogliaro, M. Bearpark, J.J. Heyd, E. Brothers, K.N. Kudin, V.N. Staroverov, T. Keith, R. Kobayashi, J. Normand, K. Raghavachari, A. Rendell, J.C. Burant, S.S. Iyengar, J. Tomasi, M. Cossi, N. Rega, J.M. Millam, M. Klene, J.E. Knox, J.B. Cross, V. Bakken, C. Adamo, J. Jaramillo, R. Gomperts, R.E. Stratmann, O. Yazyev, A.J. Austin, R. Cammi, C. Pomelli, J.W. Ochterski, R.L. Martin, K. Morokuma, V.G. Zakrzewski, G.A. Voth, P. Salvador, J.J. Dannenberg, S. Dapprich, A.D. Daniels, O. Farkas, J.B. Foresman, J.V. Ortiz, J. Cioslowski, D.J. Fox, Gaussian 09, Revision D.01, Gaussian, Inc., Wallingford CT, 2013.

[15] (a) K. Fukui, Formulation of the reaction coordinate, J. Phys. Chem. 74 (1970) 4161–4163;
(b) K. Fukui, The path of chemical reactions-the IRC approach, Acc. Chem. Res. 14 (1981) 363–368.

[16] (a) P.J. Hay, W.R. Wadt, Ab initio effective core potentials for molecular calculations. Potentials for K to Au including the outermost core orbitals, J. Chem. Phys. 82 (1985) 299–310;
(b) W.R. Wadt, P.J. Hay, Ab initio effective core potentials for molecular calculations. Potentials for main group elements Na to Bi, J. Chem. Phys. 82 (1985) 284–298.

[17] A.W. Ehlers, M. Böhme, S. Dapprich, A. Gobbi, A. Höllwarth, V. Jonas, K.F. Köhler, R. Stegmann, A. Veldkamp, G. Frenking, A set of f-polarization functions for pseudo-potential basis sets of the transition metals Sc-Cu, Y-Ag and La-Au, Chem. Phys. Lett. 208 (1993) 111–114.

[18] P.C. Hariharan, J.A. Pople, The influence of polarization functions on molecular orbital hydrogenation energies, Theor. Chim. Acta 28 (1973) 213–222.

[19] (a) Y. Zhao, N.E. Schultz, D.G. Truhlar, Exchange-correlation functional with broad accuracy for metallic and nonmetallic compounds, kinetics, and noncovalent Interactions, J. Chem. Phys. 123 (2005), 161103/1–161103/4;
(b) Y. Zhao, D.G. Truhlar, Density functionals with broad applicability in chemistry, Acc. Chem. Res. 41 (2008) 157–167;
(c) Y. Zhao, G. Truhlar, The M06 suite of density functionals for main group thermochemistry, thermochemical kinetics, noncovalent interactions, excited states, and transition elements: two new functionals and systematic testing of four M06-class functionals and 12 other functionals, Theor. Chem. Acc. 120 (2008) 215–241;
(d) Y. Zhao, D.G. Truhlar, Benchmark energetic data in a model system for grubbs II metathesis catalysis and their use for the development, assessment, and validation of electronic structure methods, J. Chem. Theory Comput. 5 (2009) 324–333.

[20] S. Grimme, J. Antony, S. Ehrlich, H. Krieg, A consistent and accurate ab initio parametrization of density functional dispersion correction (DFT-D) for the 94 elements H-Pu, J. Chem. Phys. 132 (2010), 154104/1–154104/19.

[21] L.E. Roy, P.J. Hay, R.L. Martin, Revised basis sets for the LANL effective core potentials, J. Chem. Theory Comput. 4 (2008) 1029–1031.

[22] R.E.M. Brooner, T.J. Brown, R.A. Widenhoefer, Direct observation of a cationic Gold(I)-Bicyclo [3.2.0] hept-1 (7)-ene complex generated in the cycloisomerization of a 7-phenyl-1,6-enyne, Angew. Chem. Int. Ed. 52 (2013) 6259–6261.

[23] (a) C. Shu, Y. Wang, B. Zhou, X. Li, Y. Ping, X. Lu, L. Ye, Generation of α-imino gold carbenes through Gold-catalyzed intermolecular reaction of azides with ynamides, J. Am. Chem. Soc. 137 (2015) 9567–9570;
(b) A. Zhou, Q. He, C. Shu, Y. Yu, S. Liu, T. Zhao, W. Zhang, X. Lu, L. Ye, Atom-economic generation of gold carbenes: gold-catalyzed formal [3+2] cycloaddition between ynamides and isoxazoles, Chem. Sci. 6 (2015) 1265–1271;
(c) Y. Xi, Y. Su, Z. Yu, B. Dong, E.J. McClain, Y. Lan, X. Shi, Chemoselective carbophilic addition of α-ciazoesters through ligand-controlled gold catalysis, Angew. Chem. 126 (2014) 9975–9979;
(d) Y. Duan, Y. Liu, S. Bi, B. Ling, Y. Jiang, P. Liu, Theoretical study of Gold-catalyzed cyclization of 2-alkynyl-N-propargylanilines and rationalization of kinetic experimental phenomena, J. Org. Chem. 81 (2016) 9381–9388;
(e) D. Vidhani, M. Krafft, I.V. Alabugin, Gold(I)-catalyzed allenyl cope rearrangement: evolution from asynchronicity to trappable intermediates assisted by stereoelectronic switching, J. Am. Chem. Soc. 138 (2016) 2769–2779;
(f) L. D'Amore, G. Ciancaleoni, L. Belpassi, F. Tarantelli, D. Zuccaccia, P. Belanzoni, Unraveling the anion/ligand interplay in the reaction mechanism of Gold(I)-catalyzed alkoxylation of alkynes, Organometallics 36 (2017) 2364–2376;
(g) M.E. De Orbe, L. Amenos, M.S. Kirillova, Y. Wang, V. Lopez Carrillo, F. Maseras, A.M. Echavarren, Cyclobutene vs 1,3-diene formation in the Gold-catalyzed reaction of alkynes with alkenes: the complete mechanistic picture, J. Am. Chem. Soc. 139 (2017) 10302–10311;
(h) Y. Yang, J. Li, R. Zhu, C. Liu, D. Zhang, Theoretical insight into ligand- and counterion-controlled regiodivergent reactivity in synthesis of borylated furans: 1,2-H vs 1,2-B migration, ACS Catal. 8 (2018) 9252–9261.

[24] (a) S. Kozuch, S. Shaik, How to conceptualize catalytic cycles? The energetic span model, Acc. Chem. Res. 44 (2011) 101–110;
(b) A. Uhe, S. Kozuch, S. Shaik, Automatic analysis of computed catalytic cycles, J. Comput. Chem. 32 (2011) 978–985;
(c) S. Kozuch, J.M.L. Martin, The rate-determining step is dead. Long live the rate-determining state, ChemPhysChem 12 (2011) 1413–1418.